

Diazonium Salts for Surface-Confined Visible Light Radical Photopolymerization

Idriss Bakas,^{1,2} Gorkem Yilmaz,³ Zouhair Ait-Touchente,¹ Aazdine Lamouri,¹ Philippe Lang,¹ Nicolas Battaglini,¹ Benjamin Carbonnier,⁴ Mohamed M. Chehimi,^{1,4} Yusuf Yagci³

¹Univ Paris Diderot, Sorbonne Paris Cité, ITODYS, UMR CNRS 7086, 15 Rue J-A De Baïf, Paris, 75013, France

²Equipe Matériaux Photocatalyse Et Environnement, Faculté Des Sciences, Université Ibn Zohr, B.P. 8106, Cité Dakhla, Agadir, Morocco

³Department of Chemistry, Istanbul Technical University, Maslak, Istanbul 34469, Turkey

⁴Université Paris Est, ICMPE (UMR7182), CNRS, UPEC, Thiais 94320, France

Correspondence to: M. M. Chehimi (E-mail: chehimi@icmpe.cnrs.fr) or Y. Yagci (E-mail: yusuf@itu.edu.tr)

Received 31 March 2016; accepted 20 July 2016; published online 00 Month 2016

DOI: 10.1002/pola.28241

ABSTRACT: The surface chemistry of aryl diazonium salts has progressed at a remarkable pace in the last two decades, and opened many avenues in materials science. These compounds are excellent coupling agents for polymers to surfaces via several surface-confined polymerization methods. For the first time, we demonstrate that diazonium salts are efficient for surface initiating radical photopolymerization in the visible light of methyl methacrylate (MMA) and 2-hydroxyethyl methacrylate (HEMA) taken as model monomers. To do so, 4-(dimethylamino)benzenediazonium salt was electroreduced on gold plates or flexible ITO sheets to provide 4-(dimethylamino)phenyl (DMA) hydrogen donor layers; while excited state camphorquinone acted as the free hydrogen abstractor. In the same way, we co-polymerized HEMA and MMA with ethylene glycol dimethacrylate in order to

obtain crosslinked polymer grafts. We demonstrate by XPS that gold was efficiently screened by the polymer layers and that the wettability of the surfaces accounts for the hydrophilic or hydrophobic characters of the tethered polymers. Homo- and cross-linked PMMA grafts were found to resist removal by the paint stripper methyl ethyl ketone. The grafted DMA/camphorquinone system operating in the visible light holds great promises in terms of adhesion of *in situ* designed continuous or patterned polymer coatings on various substrates. © 2016 Wiley Periodicals, Inc. *J. Polym. Sci., Part A: Polym. Chem.* **2016**, *00*, 000–000

KEYWORDS: aryl diazonium salts; camphorquinone; polymer grafts; surface-initiated radical photopolymerization; visible light

INTRODUCTION The surface chemistry of aryl diazonium salts has progressed at a remarkable pace since the last two decades,^{1–3} and opened so many new and innovative avenues in surface science in general and in materials engineering, in particular. Of relevance to the present paper, these compounds were demonstrated to be efficient coupling agents and offered various pathways to graft polymers through a broad range of substrates using a variety of surface-confined polymerization methods, namely: atom transfer radical polymerization (ATRP),^{4–7} reversible addition–fragmentation chain transfer polymerization (RAFT),⁸ radical photopolymerization,^{9,10} iniferter (initiator-transfer-terminator),^{11,12} anionic polymerization,¹³ electropolymerization,^{14–16} and chemical^{17,18} or photochemical¹⁹ oxidative polymerization of conjugated monomers.

Through accurate combinations of substrates, diazonium salts, polymerization methods and functional monomers, it became

possible to design efficient and robust systems for removal of heavy metals,²⁰ bioactive surfaces,^{21–23} electrochemical²⁴ and optical¹² sensors, and supercapacitors.²⁵ In these systems, diazonium salts have a central role as they bridge the support to the reactive and functional polymers. They appear, thus, as new items of major importance for the toolbox of the modern surface and materials chemist; this is testified by the existence of industrial products such as diazonium-modified drug eluting stents, carbon blacks and magnetic nanoparticles for theranostics.²⁶ The success of such multicomponent materials depends on the way polymers are attached. In this regard, surface-confined polymerization is attractive because it ensures grafting polymers at relatively high density, approaching near 1 chain/nm² which is actually the case for bridging polymers to surfaces through aryl layers from aryl diazonium salts.²⁷ In this case, polymer adhesion is very good and the layers withstand attack by paint removers.¹⁰

Additional Supporting Information may be found in the online version of this article.

© 2016 Wiley Periodicals, Inc.

Among the various methods applied to graft polymers on various substrate surfaces, photochemicals protocols serve significant advantages due to a wide range of ecological, energetic and financial expectations.^{28–32} These advantages include temporal control, low-energy requirements, high rates of polymerizations at ambient temperatures without the necessity of using volatile organic solvents giving rise to environmental and health-care benefits. There has been a continuous effort for the development of new photoinitiating systems with visible light sensitivity to fulfil such requirements. Among them, camphorquinone/amine system is specifically used in dental applications, as congregates nontoxicity and high initiating efficiency characteristics under low-energy radiations.²⁹ In this virtue of view, herein we report the preparation of ultrathin polymer grafts on gold surfaces under visible light irradiation for the first time, by utilizing the camphorquinone (CQ)/amine as the initiating system.

In this paper, we shall describe a new route for polymer grafts through surface-confined radical photopolymerization using *Type II* photoinitiating system: DMA groups were electrografted by electrochemical reduction to serve as hydrogen donors for the visible light excited CQ. Methyl methacrylate (MMA) and 2-hydroxyethyl methacrylate (HEMA) were photopolymerized and the resulting coatings characterized by X-ray photoelectron spectroscopy (XPS) and polarization modulation-infrared reflection-absorption spectroscopy (PM-IRRAS). To account for the stability and robustness of the coatings, we prepared crosslinked copolymers of MMA or HEMA and ethylene glycol dimethacrylate (EGDMA) and dipped the polymer-grafted gold plates in methyl ethyl ketone (MEK).

EXPERIMENTAL

Chemicals and Materials

Gold-coated glass slides (8 × 15 mm; gold thickness 55 nm) were purchased from SSens (The Netherlands), and the UV-ozone cleaner was from Boekel, Model 135500. Flexible electrodes of 300 nm-thick indium-tin-oxide (ITO) coated on 125 μm-thick poly(ethylene naphthalate), PEN, were purchased from Peccel (Kanagawa, Japan). For electrografting, we used Biologic potentiostat (model SP-150). The monomers methyl methacrylate (MMA, 100.11 g mol⁻¹, Aldrich), 2-hydroxyethyl methacrylate (HEMA, 130.14 g mol⁻¹, Aldrich), and ethylene glycol dimethacrylate (EGDMA, 198.22 g mol⁻¹, Aldrich) were purified by filtering through basic alumina column to remove the inhibitor, and then stored in the fridge before use. *N,N* dimethylaniline (DMA, Fluka), *tert*-butylnitrite (Aldrich) and camphorquinone (CQ, Ciba Specialty Chemicals product) were used as received. Acetic acid and solvents including acetonitrile (ACN), methanol (MeOH), ethanol (EtOH), dichloromethane (DCM) were from VWR ProLabo.

Synthesis of Diazonium Salt

The diazonium salt was synthesized by adding 1 mL of HBF₄ to the solution of 1 g of *N,N*-dimethyl-4-phenylenediamine

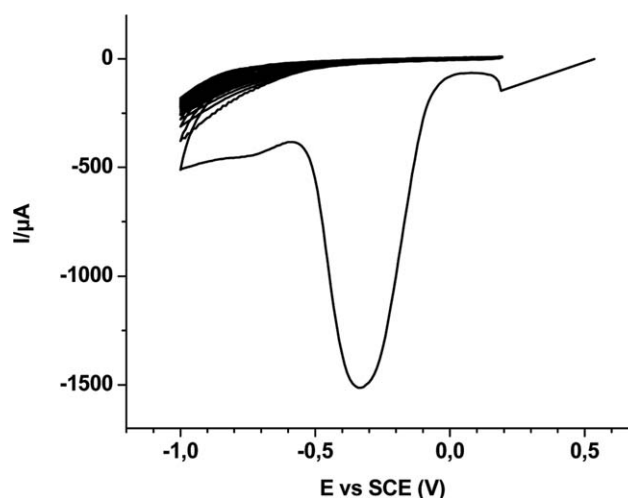


FIGURE 1 Cyclic voltammogram of a gold-coated glass slide grafted with 5 mM diazonium salt in acetonitrile +0.1 M NBu₄BF₄, $\nu = 0.2 \text{ V s}^{-1}$. Reference SCE.

in acetone. The mixture was kept in an ice bath for 10 min, then 1 mL of *tert*-butylnitrite was added dropwise at 0 °C. The solution was kept under stirring at 0 °C for 15 min. Diethyl ether was added to precipitate the diazonium salt and finally the product was recovered by filtration. The filtrate was washed with copious amounts of cold ether.

IR, cm⁻¹: (N₂⁺, 2291), (C=C_{Ar}, 1598). ¹HNMR (DMSO), δ ppm: 8.28 (d, 2H, $j = 8 \text{ Hz}$), 7.07 (d, 2H, $j = 8 \text{ Hz}$), 4.3 (s, 2H), 3.26 (s, 6H).

Electrochemical Grafting of Aryl Layers from the Diazonium Salt

The gold electrodes were ultrasonically rinsed with acetonitrile, water and ethanol, then dried in a stream of argon, cleaned in a UV-ozone cleaner and rinsed with ACN in order to remove the organic residues from the surface. The electrografting of Au slides was performed with *N,N*-dimethylbenzediazonium salt (DMA) by scanning 30 times the potential between 0.2 and -1 V. The reduction peak position obtained in the first cycle is -300 mV (Fig. 1).

We note that after one cycle the surface becomes almost passivated by the grafted aryl groups on the electrode surface. After 30 cycles, the electroreduction current vanishes and a quasi-flat response is recorded. The modified surface is noted Au-DMA. After electrografting, the surface was sonicated in ACN for 3 min, DCM and distilled water and dried under argon.

Surface-Initiated Photopolymerization (SIPP)

The polymerization reagents (Table 1) were put into a Schlenk tube (inner diameter = 9 mm) then the electrografted plates were dipped in the polymerization mixture and the reaction mixture was degassed under a stream of argon. The mixture was irradiated using a Ker-Vis blue photoreactor equipped with six lamps (Philips TL-D 18 W) emitting light nominally at 400–500 nm at room temperature for

TABLE 1 Materials Used for the Preparation of Polymer Grafts Through Aryl Layers^a

Modified Gold plates	Monomers	Crosslinker (EGDMA)	Photosensitizer (CQ)
Au-PHEMA	HEMA (1.7 mL, 1.4×10^{-2} mol)	–	1.5 mg, 9×10^{-6} mol
Au-P(HEMA/EGDMA)	HEMA (1.7 mL, 1.4×10^{-2} mol)	0.028 g, 1.4×10^{-4} mol	1.5 mg, 9×10^{-6} mol
Au-PMMA	MMA (1.7 mL, 1.6×10^{-2} mol)	–	1.5 mg, 9×10^{-6} mol
Au-P(MMA/EGDMA)	MMA (1.7 mL, 1.6×10^{-2} mol)	0.028 g, 1.4×10^{-4} mol	1.5 mg, 9×10^{-6} mol

^a All polymer grafts were prepared on Au-DMA. For the sake of simplicity, “DMA” has been removed from the abbreviations of polymer-coated gold plates.

2 h. After SIPP, the plates were washed in Soxhlet extractor for 2 h in methanol to remove the unreacted monomers, and then washed with ethanol and acetonitrile to remove organic species.

Additional preparations of polymer grafts and polymer patches were conducted in the sun simulator UVA Cube 400 equipped with a mercury lamp (Dr Honle, München, Germany) on Au-DMA and flexible ITO electrodes grafted with DMA (ITO Flex-DMA in short). The lamp-sample distance was 40 cm.

XPS Analysis

A Thermo VG Scientific ESCALAB 250 system fitted with a micro-focused, monochromatic Al K α X-ray beam (1486.6 eV, 500 μ m spot size) was used to record the spectra. The samples were stuck on sample holders using conductive double-sided adhesive tapes and outgassed in the fast entry airlock for at least 1 h at 5×10^{-8} mbar or better. The Advantage software, version 4.67, was used for digital acquisition and data processing. The pass energy was set at 40 and 100 eV for the high resolution and the survey spectra, respectively. The spectra were calibrated against the C 1s main peak component C–C/C–H set at 285 eV.

Contact Angle Measurements

Water contact angles were determined with a Krüss DSA 100 instrument (Hamburg, Germany), fitted with a drop shape analyzer.

PM-IRRAS

PM-IRRAS spectra were recorded with a Nicolet 860 FTIR (Thermo- Electron) spectrometer with a resolution of

8 cm^{-1} by adding 2000 scans with an optical mirror velocity of 0.474 cm s^{-1} .

AFM

AFM images were recorded with an NT-MDT Solver pro equipment. AFM topography was performed in the intermittent contact mode with standard silicon cantilevers. Image analysis was achieved with the free software WSxM.³³

RESULTS AND DISCUSSION

General Protocol of Surface-Confined Radical Photopolymerization on Aryl-Modified Substrates Using Camphorquinone as Hydrogen Abstractor

In previous publications we have employed grafted hydrogen donors from diazonium salts for conducting radical polymerization using benzophenone as photosensitizer capable of abstracting hydrogen from the aryl layers.^{10,22,34} In this work, we electro reduced the structurally designed diazonium salt in order to attach dimethylaminophenyl (DMA) groups as hydrogen donor species.

CQ was deliberately selected so as to provide absorption in the visible range which do not interfere with the absorption characteristics of the components of the system and damage already formed chains. Since, upon irradiation the initiating radicals are formed on the gold surface by hydrogen abstraction by the excited CQ, it is reasonable to predict that photopolymerization will be conducted at the surface gold (here Au-DMA) according to the mechanisms displayed in Figure 2.

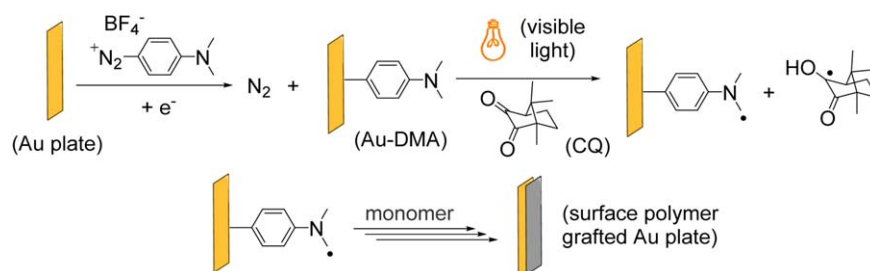


FIGURE 2 Protocol of surface-confined radical photopolymerization using grafted hydrogen donors from electroreduction of aryl diazonium salt and camphorquinone as the hydrogen donor. [Color figure can be viewed in the online issue, which is available at wileyonlinelibrary.com.]

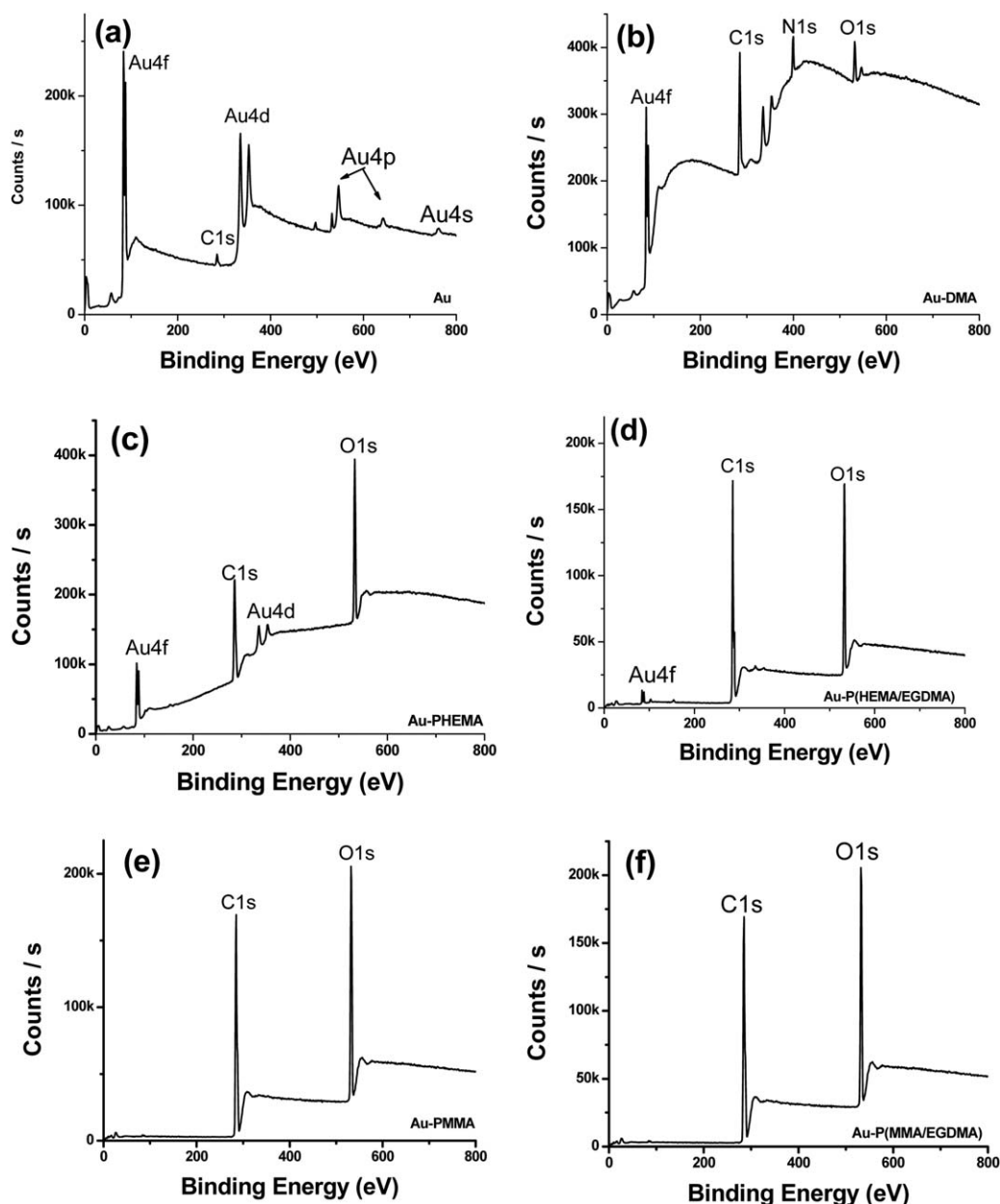


FIGURE 3 Survey spectra from (a) Au, (b) Au-DMA, (c) Au-PHEMA, (d) Au-P(HEMA/EGDMA), (e) Au-PMMA, (f) Au-P(MMA/EGDMA).

XPS

XPS was used to monitor the changes in the surface chemical composition of gold after electrografting DMA groups and making polymer grafts photopolymerization. The survey spectra are displayed in Figure 3. DMA electrografting yields a dramatic change in the inelastic background of the gold electrode [Fig. 3(a,b)]. As previously shown, there is a relative increase in the C1s peak relative to gold features. DMA has a unique elemental marker, nitrogen, as testified by the appearance of a N1s peak at ~ 399.4 eV [Fig. 3(b)] which accounts for a nitrogen atom in an aromatic amine. After photopolymerization, the surfaces display sharp C1s and O1s peaks from the polymer top layers [Fig. 3(c-f)]. The gold

features are drastically attenuated and so is the N1s peak from the DMA layer which is now sandwiched between the gold electrode and the polymer grafts.

For PHEMA grafts, crosslinking permits to attenuate a little bit more the underlying gold [Fig. 3(d)] as can be concluded from the total attenuation of Au4d in addition to those of Au4p and Au4s, whereas for the Au-PMMA and Au-P(MMA/EGDMA) there are no significant differences between the spectra displayed in Figure 3(e) and (f).

The fitted narrow regions are displayed in Figure 4. C1s spectra are displayed in Figure 4(a,b) for Au-PMMA and Au-PHEMA, respectively. The spectra are fitted with three

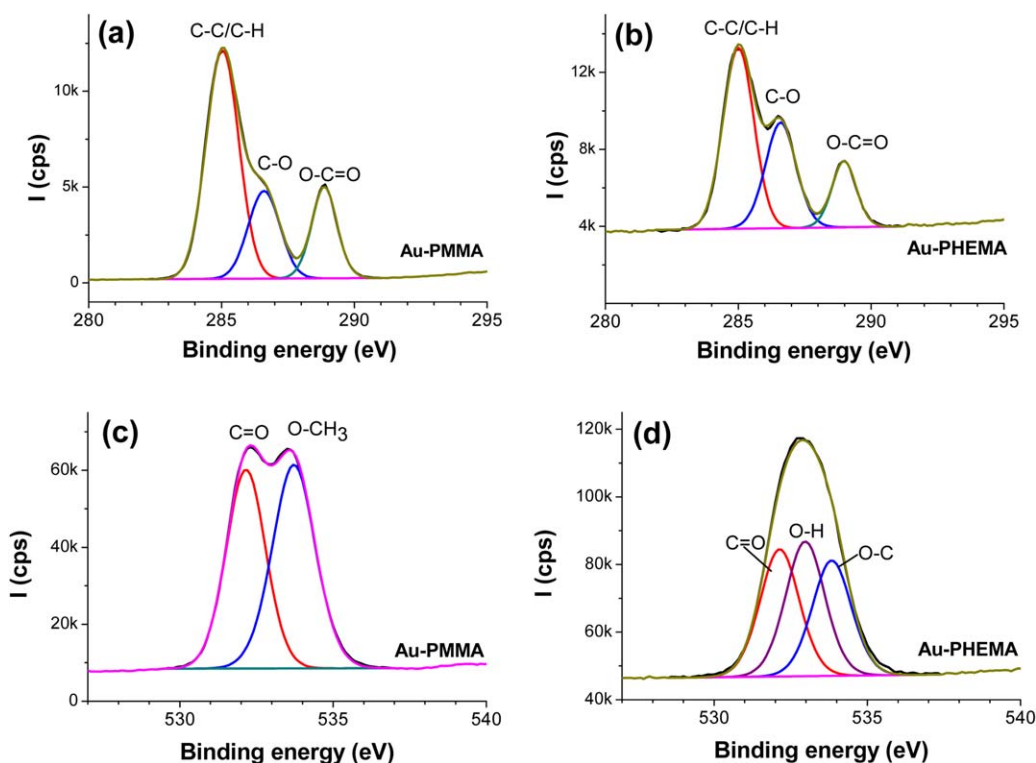


FIGURE 4 Peak-fitted C1s (a, b) and O1s (c, d) narrow regions from Au-PMMA (a, c) and Au-PHEMA (b, d). [Color figure can be viewed in the online issue, which is available at wileyonlinelibrary.com.]

components centred at 285, ~ 286.5 , and ~ 289 eV assigned to C—C/C—H, C—O, and O—C=O components, respectively. The peak components are in the 2.7/1.6/1 ratio for Au-PHEMA and 2.7/0.95/1 for Au-PMMA, which accounts for the chemical structures of the polymer grafts. Upon crosslinking, the C1s peak changes slightly for Au-P(HEMA/EDGDMA) only: the peaks are in the 3.7/1.6/1 ratio, thus indicating an increase in the contribution of the C—C/C—H bonds.

The fitted O1s regions are displayed in Figure 4 for Au-PMMA and Au-PHEMA, respectively. For PMMA graft [Fig. 4(c)], the doublet is fitted with two peaks assigned to O=C from the ester group and centred at 532.2 eV while the O—CH₃ O1s peak is centred at 533.7 eV. The O=C/O—C peak component intensity ratio is 1/1.02 matching the expected 1/1. For Au-PHEMA [Fig. 4(d)], the O1s region is fitted with three peaks centred at 532.1, 533.0, and 533.8 eV assigned to O=C, O—H, and O—C bonds. 1/1.06/0.92 matching the theoretical ratio 1/1/1. It should be noted that no significant changes were observed in peak fitting the O1s narrow regions of the crosslinked grafts.

The surface elemental compositions are reported in Table 2. The thickness of the polymer grafts was estimated from the Beer–Lambert equation applied to Au4f peak intensity:

$$I = I^{\circ} \exp(-d/\lambda)$$

where I is the intensity of the substrate characteristic peak after coating and I° is that of the substrate before coating, d

is the overlayer thickness and λ the mean free path of the photoelectron from the substrate in the top layer (about 4.1 mg m^{-2} for Au4f electrons escaping organic coatings, which is equal to 4.1 nm if one assumes a density of 1 for polymers). The homo- and crosslinked PMMA grafts are so thick that neither Au4f peaks (from the substrate) nor N1s peak (from the initiator) could be detected. So the Beer–Lambert equation above would give zero counts for I and thus an infinite value for the thickness d (d cannot be determined in this case by XPS). If one considers a rough 10 nm thickness of the polymer grafts, this corresponds to about $10 \text{ mg polymer m}^{-2}$ substrate. For a HEMA repeat unit molecular weight of 130 g mol^{-1} , the grafting density would be 46 repeat units per nm^2 which is in line with the polymeric nature of the graft.

The C/N ratio is 6.6 for Au-DMA, lower than 8 due to the existence of azo bonds (—N=N—) within the layer. After polymerization, the C/O ratios sharply decrease to 2.8 for PMMA graft and 2.2 for PHEMA which accounts for the chemical structures of the tethered polymers. Similar trends can be noted for the crosslinked polymers.

PM-IRRAS Characterisation

The IR spectra (Figs. 5 and 6) of polymers normalized to the C=O band, with or without EGDMA are close, in regard to the low amount of EGDMA added to the two monomers. Nevertheless some slight differences were observed in the C—H stretching region (3000 cm^{-1}). For PMMA (Fig. 5) in

TABLE 2 XPS-Determined Surface Chemical Composition of Untreated and Modified Gold Plates

Electrografted Surface	Au	N	C	O	Thickness (DMA or Polymer)
Au	60.4	–	31.2	8.4	
Au-DMA	6.73	11.2	73.7	8.44	8.8 nm
Au-PHEMA	2.54	0.4	67.0	30.0	4 nm
Au-P(HEMA/EGDMA)	0.47	0.24	70.1	29.2	11.2 nm
Au-PMMA	0	0	73.4	26.6	–
Au-P(MMA/EGDMA)	0	0	74.0	26.0	–

the presence of EGDMA, the latter seems to be evidenced by an additional absorption, assigned to the vibration $\nu_s(\text{OCH}_2\text{—CH}_2\text{O})$ and close to the band $\nu_s(\text{OC—H}_3)$ at 2844 cm^{-1} present both in the MMA repeat units and those mixed with EGDMA.

For the PHEMA, the intensity of this same band at 2852 cm^{-1} increases slightly in the presence of EGDMA; in the same way, the band $\nu_{\text{as}}(\text{OCH}_2\text{CH}_2\text{O})$ at 2930 cm^{-1} increases with EGDMA relatively to that $\nu_{\text{as}}(\text{CC—H}_3)$ at 2950 cm^{-1} . This suggests that the polymerized EGDMA is observed in both cases. The absence of band $\nu(\text{C=C})$ at 1640 cm^{-1} (Fig. 6) shows likely that EGDMA has polymerized with MMA and HEMA monomers. The presence of small bands at 3100 cm^{-1} $\nu(\text{H}_2\text{—C=C})$ particularly with PHEMA, could indicate that EGDMA promotes complete polymerization³⁵ but this is not confirmed by the variation of the absorption within the $\nu(\text{C=C})$ region at about 1640 cm^{-1} .

The band $\nu(\text{C=O})$ with PHEMA at 1730 cm^{-1} has a shoulder at 1705 cm^{-1} due to intramolecular hydrogen bonds C—O—H—OCH_2 . To summarize, EGDMA is well observed and has participated to the photopolymerization process.

Hydrophilic/Hydrophobic Characteristics of Gold Slides

The hydrophilic/hydrophobic properties of the Au-polymer slides were examined by water contact angles (θ_w). The drops were stable from the early stage of contact with the surfaces. Figure 7 shows qualitatively and quantitatively (see reported values in Fig. 7) that PHEMA grafts are more hydrophilic than the Au-PMMA surfaces. The average values are in line with the literature for PMMA grafts but slightly higher for PHEMA probably due to a slight contribution of DMA as gold is detected by XPS through the PHEMA top layer and thus through also DMA. For UV/ozone cleaned Au plate, the water contact angle was reported to be 35.5° ³⁶ while for aryl layer on various substrates the contact angle

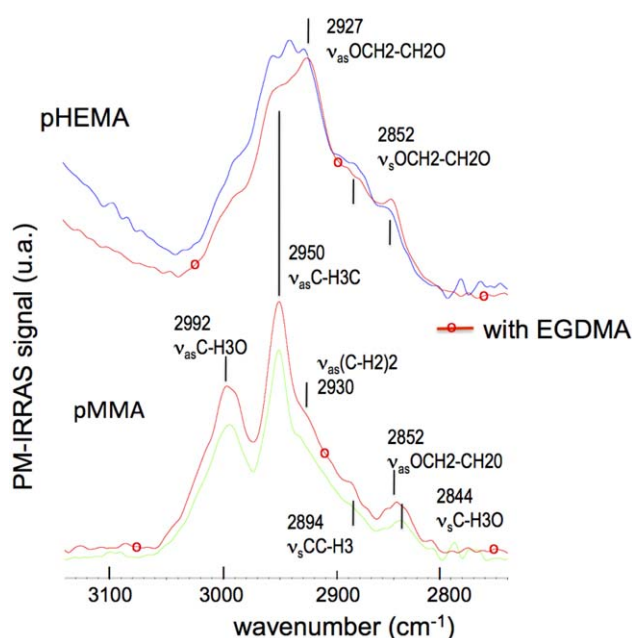


FIGURE 5 PM-IRRAS spectra of PMMA and PHEMA polymers on gold substrate with or without EGDMA in the $\nu(\text{C—H})$ region; the spectra intensities have been normalized to the $\nu(\text{C=O})$ peak intensity. [Color figure can be viewed in the online issue, which is available at wileyonlinelibrary.com.]

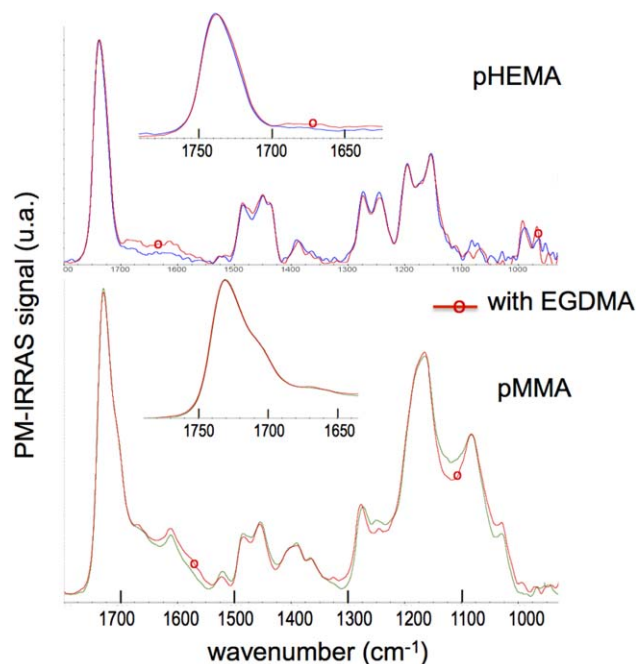


FIGURE 6 PM-IRRAS spectra of PMMA and PHEMA polymers on gold substrate with or without EGDMA in the $1700\text{—}1000\text{ cm}^{-1}$ region; zoom in of the 1700 cm^{-1} region has been inserted in both spectra. [Color figure can be viewed in the online issue, which is available at wileyonlinelibrary.com.]

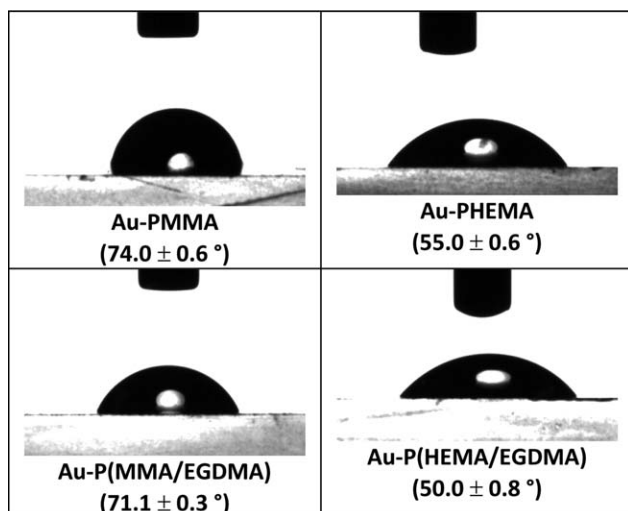


FIGURE 7 Drops of water gently deposited on polymer-coated Au surfaces.

is in the 55° to 100° range.³⁷ Interestingly, for each polymer the use of the crosslinker imparts a slight degree of relative hydrophilicity.

Adhesion Testing for Polymer Grafts

In order to demonstrate the further primacy of the described process, we interrogate adhesion of polymer grafts to gold in methyl ethyl ketone (MEK), a well-known powerful solvent for polymers,³⁸ able to swell and remove paints and varnishes.¹⁰ The plates were dipped for 60 min in MEK and then washed, dried and examined by XPS (see spectra in Supporting Information SI1). The survey spectra for the Au-PHEMA before and after dipping in MEK are quasi identical and account for PHEMA chemical composition. The cross-linked PHEMA experiences a slight leaching and the Au/C ratio increases from 0.01 to 0.03 (Table 3). For either homo- or crosslinked PMMA, the changes are marginal.

These changes induced by the solvent are not significant and indicate that the new surface photoinitiating system, in the visible light, is effective in providing polymer grafting with quasi zero leaching of polymers.

Patterned PHEMA Coating

PHEMA patches were prepared using a Teflon mask. 0.7 mm wide squares were cut from the mask to obtain windows through which simulated sunlight strikes the Au-DMA surface in contact with the polymerization solution. The mask was held with double sided adhesive copper tape. The upper side of the adhesive was screened with an aluminium foil.

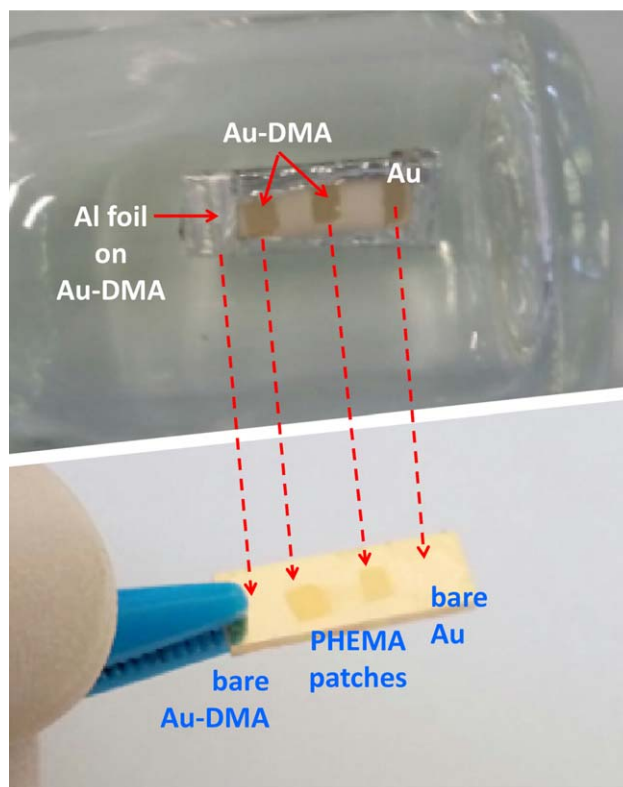


FIGURE 8 Digital photographs of Au-DMA coated with a Teflon mask (upper panel), and PHEMA patches obtained after simulated sunlight-graft polymerization on Au-DMA (lower panel). [Color figure can be viewed in the online issue, which is available at wileyonlinelibrary.com.]

Photopolymerization was conducted for 7 min and the plate was thoroughly washed as indicated for homo- and cross-linked layers.

Figure 8 shows digital photographs of an Au-DMA plate coated with the Teflon mask in the small glassy container. Bare and DMA-grafted gold areas are indicated in the upper panel. After polymerization, the lower panel shows clear squared, brown patches from the Au-DMA exposed areas. The bare Au is obviously not coated due to the absence of any initiator. The Au-DMA side that has been coated with aluminium foil retained its gold colour. Therefore, patches were vertically built only where the simulated sunlight struck the Au-DMA exposed regions.

The patches were scanned by XPS. 30 spots were analyzed with a 200 μm-sized X-ray spot, and the step was 244 μm. Figure 9 shows 3D image of Au4f spectra. At the extreme

TABLE 3 Au/C Atomic Ratio Determined for Polymer-Coated Surfaces Before and After Dipping in Methyl Ethyl Ketone for 60 Min

	Au-PMMA	Au-P(MMA/EGDMA)	Au-PHEMA	Au-P(HEMA/EGDMA)
Pristine	0	0	0.04	0.01
Dipped in MEK	0.005	0.0005	0.04	0.03

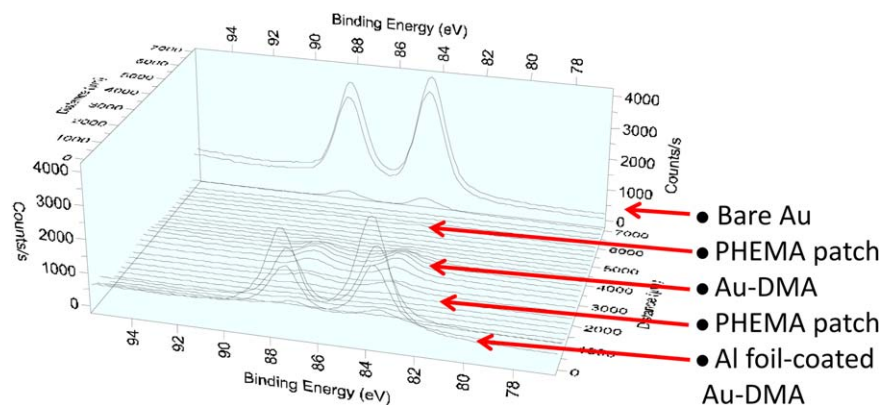


FIGURE 9 3D display of Au 4f spectra taken along the main axis of the slide decorated with two PHEMA patches. X-ray spot = 200 μm ; displacement = 244 μm . [Color figure can be viewed in the online issue, which is available at wileyonlinelibrary.com.]

points the Au4f peak is intense while in between moderate intense peaks appear where the Au-DMA slide was screened by the Teflon mask. The XPS analysis over a long distance of ~ 7.1 mm indicates the possibility of patterning surfaces with the actual process. The thickness in the middle of the left hand side PHEMA patch in Figure 8, lower panel, was estimated to be 23 nm using Beer–Lambert equation.

The patches were imaged by AFM to estimate both the topography of the polymer and its thickness. We have taken advantage of the presence of a scratch defect in Figure 10(a) to measure the thickness. Note however that scratched continuous PHEMA patches gave similar results at about a thickness of ~ 30 nm [Fig. 10(b)]. This is in fair agreement with XPS determined thickness of 23 nm for the left hand side patch shown in Figure 8, lower panel.

The surface roughness (RMS value) is 22 ± 2 nm measured on a $30 \mu\text{m} \times 30 \mu\text{m}$ scratch-less area. This value is fairly high, as the measure integrates the bright protrusions (probably polymer particles) spread out everywhere on the patch itself.

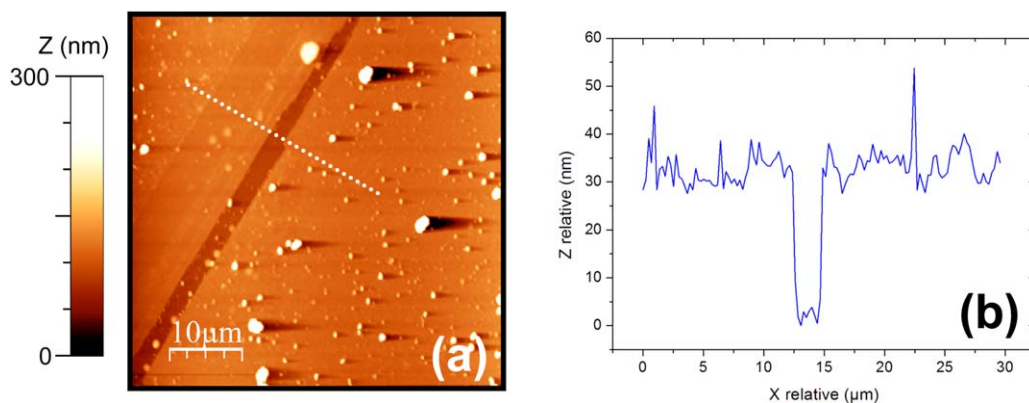


FIGURE 10 AFM topographic image of a PHEMA patch showing densely grafted coating (a). Relative Z heights are plotted versus displacement in (b). Height measurements were determined along the white dotted line in (a). Scanned region: $50 \times 50 \mu\text{m}^2$. [Color figure can be viewed in the online issue, which is available at wileyonlinelibrary.com.]

Other Substrate/Polymer System: Flexible ITO Grafted with PHEMA

So far we have considered gold as a substrate for homopolymer, copolymer, and patterned homopolymer grafts. The grafted DMA/CQ initiating system is versatile and was extended to a flexible ITO electrode (ITO-coated PEN sheet, hereafter ITO Flex). The ITO was electrografted with DMA prior to photopolymerization in the UVA Cube 400 sun simulator for 7 min in the conditions reported in Table 1.

Figure 11(a) shows survey spectra from ITO Flex, ITO Flex-DMA, and ITO Flex-PHEMA; the latter was prepared using the sun simulator as a source of visible light. In Figure 11(b), line scan of the same electrode is displayed and shows survey [Fig. 11(b)] and narrow C1s regions [Fig. 11(c)].

Figure 11(a) shows the efficient electrografting process as N1s appears in the survey spectrum of ITO Flex-DMA and a concave background appears which accounts for partial screening of ITO by the DMA grafted layer. The intensity of the C1s peak increases too compared to those from the underlying substrate (In4d, In3d, Sn3d, and O1s). After SIPP,

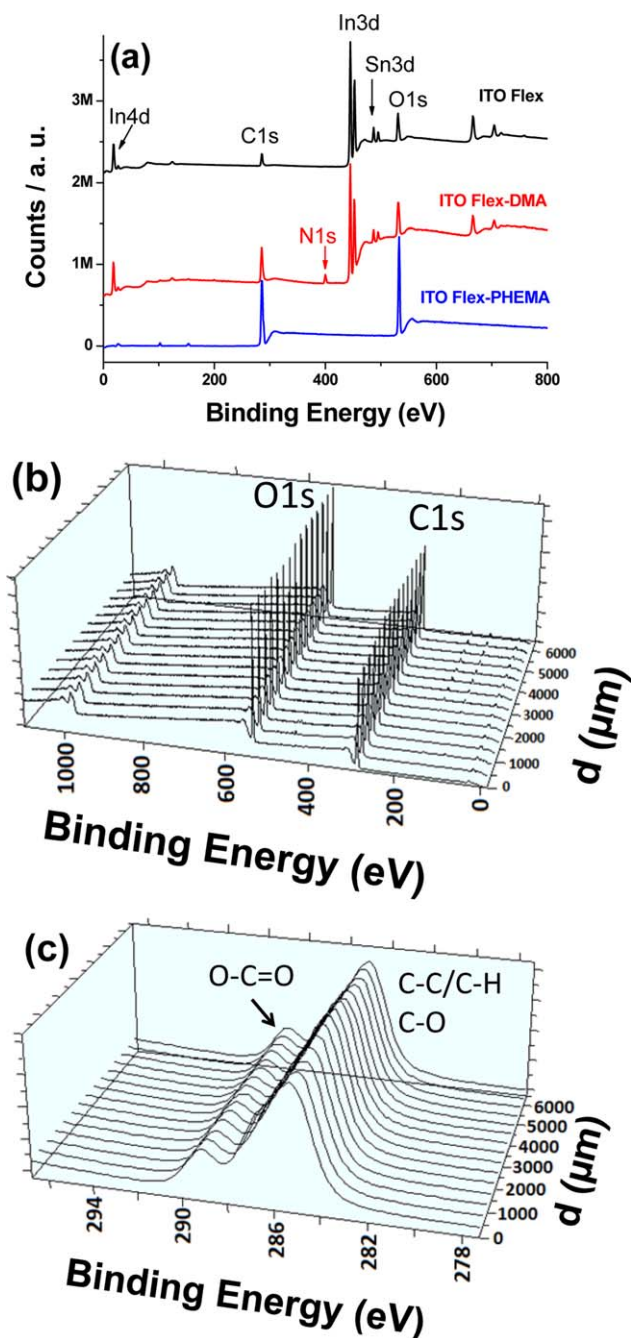


FIGURE 11 (a) Survey spectra from ITO Flex, ITO Flex-DMA and ITO Flex-PHEMA; (b) survey spectra taken from 15 points on ITO Flex-PHEMA; (c) C1s regions taken from 15 points on ITO Flex-PHEMA. XPS analysis conditions: X-ray spot = 400 μm ; step size = 452 μm ; total distance for line scan = 6328 μm . [Color figure can be viewed in the online issue, which is available at wileyonlinelibrary.com.]

the survey spectrum displays only sharp C1s and O1s peaks from PHEMA indicating very efficient attachment of PHEMA on flexible ITO. The C/O atomic ratio is 2.25 and matches the expected one for PHEMA. In addition, the C1s from ITO Flex-PHEMA was fitted with three components as that shown in Figure 4(b) for Au-PHEMA.

We have scanned the same substrate in XPS and the 15 survey [Fig. 11(b)] and C1s [Fig. 11(c)] spectra are identical, indicating a homogeneous coating over a distance of ~ 6.3 mm. The C/O atomic ratio along the scanned line is 2.30 ± 0.05 which accounts for an excellent homogeneity of the coating on flexible ITO. The ITO peaks were absent indicating thick coating; however on a few spots we could record very noisy N1s peaks from the underlying DMA initiator layer. Taking into account a mean free path of about 3.6 nm for N1s traveling through an organic top layer and taking into account the N1s peak intensity from ITO Flex-DMA and ITO Flex-PHEMA, we estimated the minimal thickness of PHEMA grafts to 14 nm. For other sites, N1s was not distinguishable from the noise indicating a much higher thickness.

CONCLUSIONS

Homo- and crosslinked PMMA and poly(2-hydroxyethyl methacrylate) (HEMA) were grafted to gold through surface-confined radical photopolymerization in the visible light. DMA groups were electrografted by electrochemical reduction to serve as hydrogen donors for photoexcited camphorquinone (CQ). The changes in the chemical composition of gold slides were monitored by XPS and PM-IRRAS whereas the hydrophilic character was investigated by means of contact angle measurements. Both XPS and PM-IRRAS analyses indicate a dense layer of the hydrophilic (PHEMA) and hydrophobic (PMMA) polymers. As proved by AFM, thickness could reach 30 nm (for PHEMA) under simulated sunlight polymerization conditions. We have also considered adhesion aspects of polymer grafts for coated slides dipped in the very well-known paint remover, methyl ethyl ketone (MEK) solvent. The grafted DMA/CQ appears as a very efficient photoinitiating system as it provides polymer grafts with very good adhesion and resistance to leaching in methyl ethyl ketone solvent. In addition to these conceptual aspects, it is demonstrated that the new photoinitiating system permits to obtain patterned polymer coating on gold and that it can be extended to other substrates as demonstrated with flexible ITO electrodes. The results obtained so far show that this new protocol combining diazonium salt and photopolymerization using CQ as a visible light photosensitizer is a new, fast, and elegant way to prepare ultrathin functional polymer grafts with excellent adhesion to various substrates, either as continuous or patterned coatings.

ACKNOWLEDGMENTS

All authors are indebted to the ANR for provision of financial support through the ANR project POLARISafe (No ANR-12-SECU-011-01).

REFERENCES AND NOTES

- 1 Aryl Diazonium Salts: New Coupling Agents in Polymer and Surface Science; M. M. Chehimi, Ed.; © 2012 Wiley-VCH: Weinheim, Germany (ISBN: 978-3-527-32998-4).

- 2 J. Pinson, F. Podvorica, *Chem. Soc. Rev.* **2005**, *34*, 429–439.
- 3 D. Bélanger, J. Pinson, *Chem. Soc. Rev.* **2011**, *40*, 3995–4048.
- 4 T. Matrab, M. M. Chehimi, C. Perruchot, A. Adenier, V. Guillez, M. Save, B. Charleux, E. Cabet-Deliry, J. Pinson, *Langmuir* **2005**, *21*, 4686–4694.
- 5 T. Liu, R. Casado-Portilla, J. Belmont, K. Matyjaszewski, *J. Polym. Sci. A: Polym. Chem.* **2005**, *43*, 4695–4709.
- 6 M. Lillethorup, K. Torbensen, M. Ceccato, S. Uttrup Pedersen, K. Daasbjerg, *Langmuir* **2013**, *29*, 13595–13604.
- 7 A. Jacques, B. Barthelemy, J. Delhalle, Z. Mekhalif, *J. Electrochem. Soc.* **2015**, *162*, G94–G102.
- 8 G. J. Wang, S. Z. Huang, Y. Wang, L. Liu, J. Qiu, Y. Li, *Polymer* **2007**, *48*, 728–733.
- 9 S. Gam-Derouich, B. Carbonnier, M. Turmine, P. Lang, M. Jouini, D. Ben Hassen-Chehimi, M. M. Chehimi, *Langmuir* **2010**, *26*, 11830–11840.
- 10 S. Gam-Derouich, S. Mahouche-Chergui, M. Turmine, J. Y. Piquemal, D. Ben Hassen-Chehimi, M. Omastová, M. M. Chehimi, *Appl. Surf. Sci.* **2011**, *605*, 1889–1899.
- 11 Z. Salmi, S. Gam-Derouich, S. Mahouche-Chergui, M. Turmine, M. M. Chehimi, *Chem. Pap.* **2012**, *66*, 369–391.
- 12 R. Ahmad, N. Félijd, L. Boubekour-Lecaque, S. Lau-Truong, S. Gam-Derouich, P. Decorse, A. Lamouri, C. Mangeney, *Chem. Commun.* **2015**, *51*, 9678–9681.
- 13 J. M. Tour, J. L. Hudson, R. Krishnamoorti, K. Yurelki, C. A. Mitchell, Polymerization Initiated at the Sidewalls of Carbon Nanotubes, WO/2005/030858, **2005**.
- 14 J.-C. Lacroix, J. Ghilane, L. Santos, G. Trippé-Allard, P. Martin, H. Randriamahazaka, In ref. 1, Chap. 8, pp 181–195.
- 15 A. Blacha, P. Koscielniak, M. Sitarz, J. Szuber, J. Zak, *Electrochim. Acta* **2012**, *62*, 441–446.
- 16 A. Blacha-Grzechnik, R. Turczyn, M. Burek, J. Zak, *Vib. Spectrosc.* **2014**, *71*, 30–36.
- 17 A. Mekki, S. Samanta, A. Singh, Z. Salmi, R. Mahmoud, M. M. Chehimi, D. K. Aswal, *J. Colloid Interface Sci.* **2014**, *418*, 185–192.
- 18 K. Jlassi, S. C. C. Kurup, M. A. Poothanari, M. Benna-Zayani, S. Thomas, M. M. Chehimi, *Langmuir* **2016**, *32*, 3514–3524.
- 19 S. Samanta, I. Bakas, A. Singh, D. K. Aswal, M. M. Chehimi, *Langmuir* **2014**, *30*, 9397–9406.
- 20 J. P. Jin, Y. Fu, X. C. Bao, X. S. Feng, Y. Wang, W. H. Liu, *J. Appl. Electrochem.* **2014**, *44*, 621–629.
- 21 S. Gam-Derouich, M. Gosecka, S. Lepinay, M. Turmine, B. Carbonnier, T. Basinska, S. Slomkowski, M. C. Millot, A. Othmane, D. Ben Hassen-Chehimi, M. M. Chehimi, *Langmuir* **2011**, *27*, 9285–9294.
- 22 S. Gam-Derouich, A. Lamouri, C. Redeuilh, P. Decorse, F. Maurel, B. Carbonnier, S. Beyazit, G. Yilmaz, Y. Yagci, M. M. Chehimi, *Langmuir* **2012**, *28*, 8035–8045.
- 23 Z. Salmi, A. Lamouri, P. Decorse, M. Jouini, A. Boussadi, J. Achard, A. Gicquel, S. Mahouche-Chergui, B. Carbonnier, M. M. Chehimi, *Diamond Relat. Mater.* **2013**, *40*, 60–68.
- 24 A. Khelifi, S. Gam-Derouich, M. Jouini, R. Kalfat, M. M. Chehimi, *Food Control.* **2013**, *31*, 379–386.
- 25 X. Wang, T. Wang, C. Yang, H. Li, P. Liu, *Appl. Surf. Sci.* **2013**, *287*, 242–251.
- 26 A. A. Mohamed, Z. Salmi, S. A. Dahoumane, A. Mekki, B. Carbonnier, M. M. Chehimi, *Adv. Colloid Interface Sci.* **2015**, *225*, 16–36.
- 27 T. Matrab, M. Save, B. Charleux, J. Pinson, E. Cabet-Deliry, A. Adenier, M. M. Chehimi, M. Delamar, *Appl. Surf. Sci.* **2007**, *601*, 2357–2366.
- 28 Y. Yagci, W. Schnabel, *Prog. Polym. Sci.* **1990**, *15*, 551–601.
- 29 Y. Yagci, S. Jockusch, N. J. Turro, *Macromolecules* **2010**, *43*, 6245–6260.
- 30 T. Zhang, T. Chen, I. Amin, R. Jordan, *Polym. Chem.* **2014**, *5*, 4790–4796.
- 31 N. Marchyk, J. Maximilien, S. Beyazit, K. Haupt, B. T. S. Bui, *Nanoscale* **2014**, *6*, 2872–2878.
- 32 A. Vitale, M. Sangermano, R. Bongiovanni, P. Burtscher, N. Moszner, *Materials* **2014**, *7*, 554–562.
- 33 I. Horcas, R. Fernández, J. M. Gómez-Rodríguez, J. Colchero, J. Gómez-Herrero, A. M. Baro, *Rev. Sci. Instrum.* **2007**, *78*, 013705.
- 34 I. Bakas, Z. Salmi, M. Jouini, F. Geneste, I. Mazerie, D. Floner, B. Carbonnier, Y. Yagci, M. M. Chehimi, *Electroanalysis* **2015**, *27*, 429–439.
- 35 C. W. Huang, Y. M. Sun, W. F. Huang, *J. Polym. Sci. A: Polym. Chem.* **1997**, 1873–1889.
- 36 B. Mrabet, A. Mejbri, S. Mahouche, S. Gam-Derouich, M. Turmine, M. Mechouet, P. Lang, H. Bakala, M. Ladjimi, A. Bakhrouf, S. Tougaard, M. M. Chehimi, *Surf. Interface Anal.* **2011**, *43*, 1436–1443.
- 37 K. Hinrichs, K. Roodenko, J. Rappich, M. M. Chehimi, J. Pinson, In ref. 1, Chap. 4, pp 71–101.
- 38 B. A. Miller-Chou, J. L. Koenig, *Prog. Polym. Sci.* **2003**, *28*, 1223–1270.